Chem-Bio Informatics Journal, Vol. 3, No. 1, pp.1-11(2003)

Molecular Dynamics Simulations of Prion Proteins - Effect of Ala^{117}→Val mutation-

Noriaki Okimoto[1]*, Kazunori Yamanaka[2], Atsushi Suenaga[3], Yoshinori Hirano[1], Noriyuki Futatsugi[3], Tetsu Narumi[3], Kenji Yasuoka[4], Ryutaro Susukita[1], Takahiro Koishi[1], Hideaki Furusawa[1], Atsushi Kawai[1], Masayuki Hata[2], Tyuji Hoshino[2], and Toshikazu Ebisuzaki[1]

[1]*Advanced Computing Center, Computational Science Division, Institute of Physical and Chemical Research (RIKEN), 2-1 Hirosawa, Wako-shi, Saitama 351-0198, Japan*
[2]*Graduate School of Pharmaceutical Sciences, Chiba University, 1-33 Yayoi-cho, Inage-ku, Chiba-shi, Chiba 263-8522, Japan*
[3]*Genomic Sciences Center, Institute of Physical and Chemical Research (RIKEN), E-503, 214 Maeda, Totsuka-ku, Yokohama-shi, Kanagawa 224-0804, Japan*
[4]*Keio University Department of Mechanical Engineering, 3-14-1 Hiyoshi, Kouhoku-ku, Yokohama-shi, Kanagawa 223-8521, Japan*

**E-mail: okimoto@atlas.riken.go.jp*

(Received October 24, 2002 ; accepted January 10,2003 ; published online February 28,2003)

Abstract

We investigated the conformational change in the human prion protein owing to an Ala^{117}→Val mutation by using molecular dynamics simulations. This mutation is related to Gerstmann-Sträussler-Sheinker disease, one of the familial prion diseases. Five prion protein structures were simulated in the periodic or non-periodic system. The results of molecular dynamics calculations indicated that the globular domains of wild-type structures (109-228 and 90-228) were stable. In contrast, the globular domains of mutant structures (109-228 and 90-228) were sensitive to the N-terminal region possessing the Ala^{117}→Val mutation, and the β-sheet regions were increased.

Key Words: Molecular Dynamics Simulation, Prion Protein, Gerstmann-Sträussler-Sheinker disease, Molecular Dynamics Machine

Area of Interest: Molecular Computing

1. Introduction

Prion diseases are manifested as familial, infectious, or sporadic diseases, and they cause neurodegenerative disorders such as kuru, Creutzfeldt-Jacob disease (CJD), Gerstmann-Sträussler-Sheinker syndrome (GSS), and fatal familial insomnia (FFI) in humans and scrapie and bovine spongiform encephalopathy (BSE) in animals [1]. These disorders are thought to be caused by the transformation of a normal prion protein (PrP^{C}) into an abnormal prion protein (PrP^{SC}), which accumulates in plaques in the brain [2]. PrP^{C} has one disulfide bridge and is anchored to the cell membrane via a glycosyl phosphatidyl inositol anchor [3] [4]. The important point is that no chemical difference between PrP^{C} and PrP^{SC} has been identified [5]. Nevertheless, experiments using circular dichroism and Fourier-transform infra-red analyses have shown that PrP^{C} has a low β-sheet content (about 3 %) and is sensitive to proteases, while PrP^{SC} has a high β-sheet content (about 30 %) and is protease-resistant [5] [6]. Recently, NMR experiments have revealed the three-dimensional structures of bovine prion protein [7] and human prion protein HuPrP [8], both of which correspond to PrP^{C}. These structural data have indicated that the N-terminal region (up to approximately 125) is flexible, and that the C-terminal region containing the globular domain (125-228) is rigid. The globular domain consists of three α-helices and a short antiparallel β-sheet (see Figure 1).

Figure 1. Potential energy-minimized structure of the NMR-determined parts of HuPrP.

Most cases of human prion diseases occur spontaneously from unknown causes. However, familial prion diseases such as GSS, FFI, and CJD are related to distinct point mutants within the human gene of PrP^{C} (PRNP) [9] [10]. Point mutations in the PRNP gene are seen in positions 102, 105, 117, 145, 198, and 217 in GSS and 178, 200, and 210 in most cases of CJD. Some mutations related to GSS occur in only a few families [11] [12] [13]; e.g., the P102L mutation was detected in more than 30 families, whereas the A117V mutation was detected in only three families [14]. It is interesting that the A117V mutation requires two changes in the genetic code to generate an amino acid change. Other experiments on peptides with the A117V mutation have suggested that the β-sheet content would increase [15]. In the current work, focusing on the A117V mutation, we tried to elucidate the correlation between the A117V mutation and prion protein (PrP) structure by using molecular dynamics (MD) calculations. The MD calculations were applied to two different types of systems (periodic and non-periodic systems). The former was performed by using a cutoff technique (14 Å), and the latter was executed without the cutoff by using a special purpose computer, Molecular Dynamics Machine (MDM) [16].

2. Methods

2.1 Construction of Initial Structure

We prepared five HuPrP initial structures (three for the periodic system and two for the non-periodic system). These structures are classified into 3 kinds of models. These three models were constructed as follows. Model 1 was derived from the NMR structures of HuPrP (125-228) [8]. This model was simulated only for the periodic system and included a globular domain of PrP^C. We called this model a "control structure." Model 2 was constructed by adding an extra peptide chain containing 117Ala (109-124 for the periodic system and 90-124 for the non-periodic system) to Model 1 (see Figure 2). We called this model a "wild-type structure." Model 3 was constructed by adding an extra peptide chain containing 117Val (109-124 for the periodic system and 90-124 for the non-periodic system) to Model 1(see Figure 2). We called this model a "mutant structure." The wild-type extra peptides above were built to be a straight chain because the parts were too flexible and disordered to be generated properly via the homology modeling. The mutant extra peptide was modeled by replacing Ala with Val at residue 117.

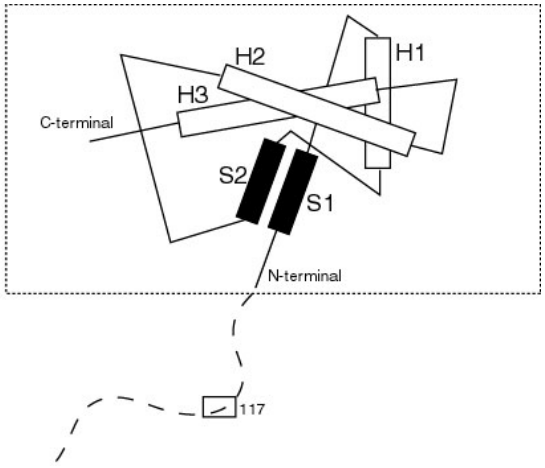

Figure 2. Construction of model structures.
The control structure (NMR-determined structure) is enclosed by a rectangle. The control structure containing the globular domain consists of three α-helices (H1, H2, and H3) and a short β-sheet (S1 and S2). In the wild-type and mutant structures, the extra peptide chain is indicated by a broken line.

2.2 Details of Computation

Molecular mechanics (MM) potential energy minimizations and MD simulations were carried out under both periodic and non-periodic boundary conditions. The computation details are shown in Table 1. The number of solvent water molecules in each system is shown in Table 2. The pH of every protein was set at neutral and each system included no ions.

Table 1. Computation details.

	Periodic system	Non-periodic system
Program	Amber 5.0 [17]	Modified Amber6.0 [18] for MDM
Force field parameters	Parm94 [19]	Parm96 [20]
Solvent*	Rectangular box (Minimum thickness of solvent shell is 12 Å)	Sphere (Radius = 72 Å)
Time step	1 fs	
Temperature control	Berendsen algorithm [21] with coupling time of 0.2 ps.	
Bond length constraints	Only bonds involving hydrogen were constrained.	
Pressure control	Applied.	Not applied.
Non-bonded interactions	Cutoff method (14 Å) was used.	All interactions were calculated
Simulation time (300 K)	2 ns	5 ns

*TIP3P water model [22].

Table 2. Number of solvent water molecules in each system.

	Periodic system	Non-periodic system
Control	9025	-
Wild-type	12336	48881
Mutant	12426	48875

2.3 Strategy of Simulations

The procedure used in our simulations is as follows. First, potential energy minimizations were performed on each of the initial systems. In case of the wild-type and mutant structures, minimizations were executed only for the extra peptide chains and solvent water molecules. Then, the respective whole systems were minimized. Next, MD simulations were performed on the energy-minimized systems. In the system of the control structure, after a 10-ps MD simulation at 600 K only for solvent water molecules, the whole systems were gradually heated to 300 K for 70 ps and then kept at 300 K for the next 2 ns. In the systems of the wild-type and mutant structures, after the annealing calculations (5 ps at 0.1K, 20 ps at 600 K, 5 ps at 300 K, and 5 ps at 5K) only for the extra peptide chains and solvent water molecules (to remove the arbitrariness for the extra peptide chains of the N-terminal region), the whole systems were gradually heated to 300 K for 70 ps, and then the temperatures were kept at 300 K for the next 2 ns or 5 ns. The trajectories at 300 K were considered to be the most probable structures under physiological conditions and were analyzed in detail.

Secondary structures were analyzed by using PROCHECK [23], and the images of simulated prion proteins were generated with MOLMOL [24].

3. Results

3.1 RMSD and Residue-based RMSD

Periodic system. Figure 3 ((a) and (b)) shows the root mean square deviations (RMSDs) of the whole protein (109-228) and globular domains (125-228) of the HuPrP models. The RMSD of the control structure was kept at 3 Å for 2 ns, which indicated that the globular domain was rather stable. The RMSDs of the whole wild-type and mutant structures increased rapidly within 200 ps and then fluctuated at 6-7 Å. In addition, the RMSD of the globular domain of the wild-type structure was maintained at approximately 3 Å for 2 ns similarly as in that control structure. In contrast, the RMSD of the globular domain of the mutant structure gradually increased and fluctuated at 5-6 Å after 1 ns. These data on periodic systems revealed that the large RMSD of the whole wild-type structure arose not from the structural change in the globular domain but from the structural change in the extra peptide chain of the N-terminal region. In contrast, the large RMSD of the whole mutant structure was due not only to the structural change in the extra peptide chain of the N-terminal region but also to the drastic structural change in the globular domain.

Non-periodic system. Figure 3 ((c) and (d)) shows the RMSDs of the whole protein (90-228) and globular domains (125-228) in non-periodic systems. The RMSDs of whole structures increased rapidly and then reached approximately 10 Å, while the curve of the mutant type was always slightly above that of the wild-type. With regard to the RMSD of the globular domain, the value within the first 2 ns of the mutant structure was larger than that of the wild-type structure, and the values within the final 3 ns of both structures were equilibrated at 2.5 Å. These data seemed to indicate that the extra peptide of the mutant structure influenced the globular domain within 2 ns. We cannot conclude that definitely, however, because the RMSD is a mere indicator of the difference in structure from that of the standard.

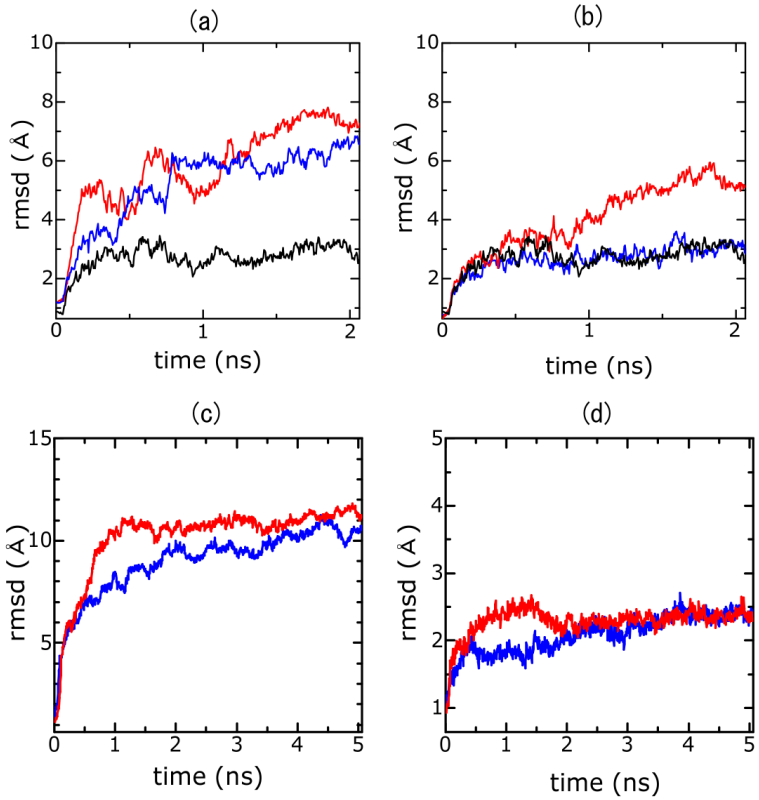

Figure 3. Root-mean-square deviations (RMSDs) of the main chain atoms.
(a) RMSD of the whole protein in the periodic system, (b) RMSD of the globular domain in the periodic system, (c) RMSD of the whole protein in the non-periodic system, and (d) RMSD of the globular domain in the non-periodic system. Black, blue, and red lines indicate RMSDs of the control, wild-type, and mutant structures, respectively. With regard to the initial structures of the MD simulations (after annealing), there were no notable differences among the whole structures (1.2 and 1.9 Å for RMSDs on the main chain atoms between wild-type and mutant models in both periodic and non-periodic systems). The ordinate is RMSD (Å) and the abscissa is time (ps).

3.2 MD simulation structures

Periodic system. The average structure of the control structure is shown in Figure 4(a). This figure indicates that the globular domain containing three α-helices and a short antiparallel β-sheet is stably maintained. The secondary structures of the control structure were similar to those of the NMR structure, although the α-helix at the C-terminal side of H3 was slightly transformed into a 3_{10}-helix after 1.5 ns (see Figure 6). Accordingly, the control structure was concluded to be stably maintained for the 2 ns MD simulation.

A noticeable feature of the average structure of the wild-type structure was that the extra peptide chain in the N-terminal region, which was a disordered strand at the initial state of MD simulation, formed a new α-helix (see Figure 5(b)). This extra peptide chain began to form α- and 3_{10}-helices at around 700 ps, and then the new α-helix was almost completed at 2 ns. It was also observed that H1 was deformed and somewhat unstable. The parts other than H1 in the globular domain maintained almost the initial structure. Analysis of the secondary structure (Figure 6) also

indicated that H1 changed from an α-helix to a 3_{10}-helix and then became unstable. This flexibility of H1 is supported by NMR experiments [7]. The H2, H3, and short antiparallel β-sheet in the globular domain were stably maintained for 2 ns similarly as in the control structure (see Figure 6).

An interesting finding from the MD simulation of the mutant structure was that the original antiparallel β-sheet had been extended. The average structure (Figure 4(c)) clearly indicated the extension of the β-sheet. Analysis of the secondary structures (see Figure 6) indicated that the extension of the β-sheet occurred from 1 ns, and that the span of the β-sheet (8.12 residues) was approximately two-times greater than those of the control and wild-type structures (3.67 and 4.65 residues, respectively). The H1 region, which is between S1 and S2, was deformed with this extension of the original β-sheet, and, as a consequence, the central part of H1 collapsed (Figure 4(c)).

Non-Periodic system. We can also observe the remarkable structural change that the originally short antiparallel β-sheet expanded twofold in the mutant structure after 1 ns (see Figures 5(b) and 7). On the one hand, parts other than those in the vicinity of the antiparallel β-sheet in the globular domain are similar to the initial and NMR structures. On the other hand, the globular domain of the wild-type structure is very similar to the initial and NMR structures (see Figures 5(a) and 7). Namely, with regard to the globular domain, there was little difference between the wild-type and mutant structures except in the vicinity of the β-sheet. The β-sheet, consisting of S1 and S2, would be sensitive to the conformation of the extra peptide of the N-terminal, which links to S1. A conformational difference is seen between the wild-type and mutant extra peptides (90-124), especially near the S1 and N-terminal. We speculate that the expansion of the β-sheet or the paralleling of two β-strands is associated with the conformation of the region near S1; although this structural change without the destruction of H1 is too subtle to be reflected in the RMSD value (see Figure 3).

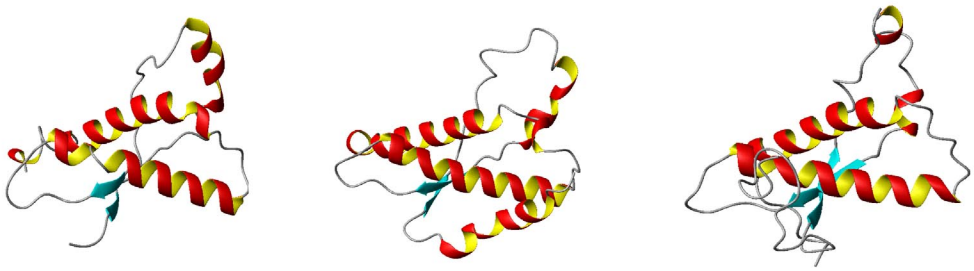

Figure 4. Average structures of HuPrP models in periodic systems.
((a) control structure, (b) wild-type structure, and (c) mutant structure). These structures were obtained from the final 1 ns MD simulations.

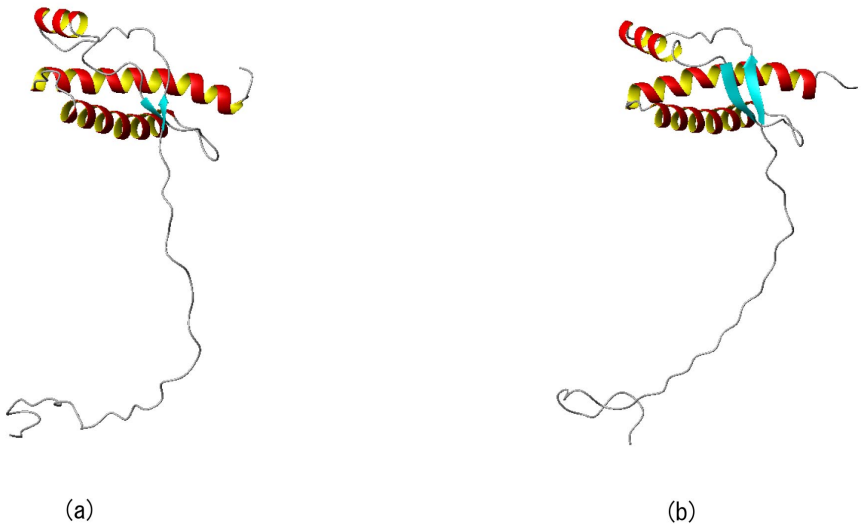

Figure 5. Average structures of HuPrP models in non-periodic systems.
((a) wild-type structure and (b) mutant structure). These structures were obtained from the final 1 ns MD simulations. The viewpoint is from the back of Figure 4.

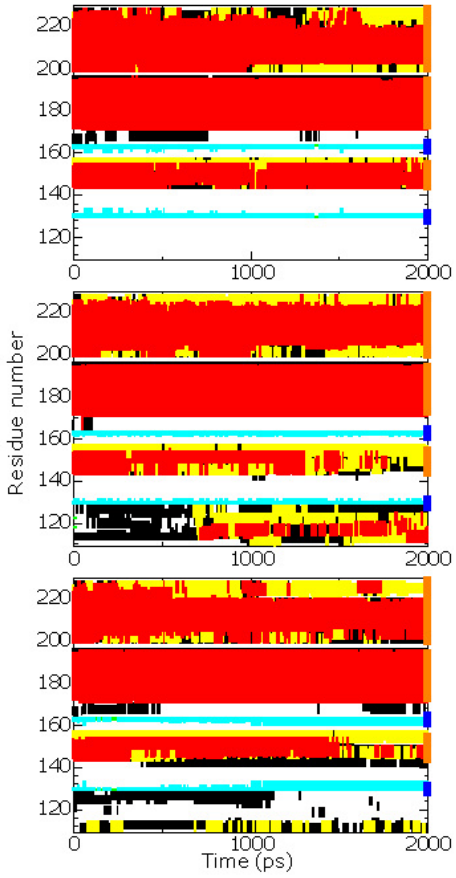

Figure 6. Secondary structure as a function of simulation time.
The top Figure shows the control structure; middle figure, the wild-type structure; and bottom figure, the mutant structure. The α-helix is shown as a red box, 3_{10}-helix as a yellow box, β-sheet as a blue box, β-bridge as a green box, and a turn as a black box.

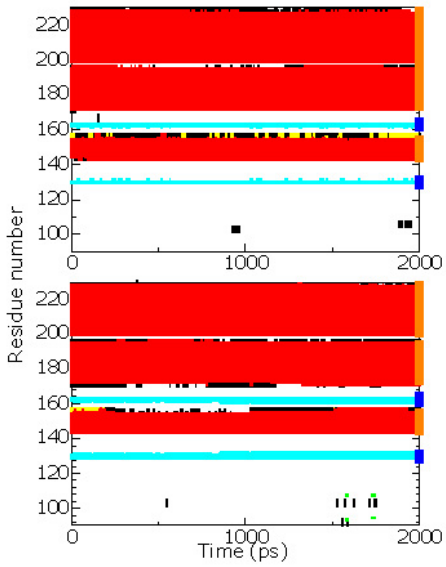

Figure 7. Secondary structure as a function of simulation time (first 2 ns).
The top figure shows the wild-type structure and the bottom figure the mutant structure. The final 3 ns of data are not shown, because they are very similar to the first 2 ns of data. The α-helix is shown as a red box, 3_{10}-helix as a yellow box, β-sheet as a blue box, β-bridge as a green box, and a turn as a black box.

4. Discussion

In the current study, we performed MD simulations of periodic and non-periodic systems. Our periodic systems dealt with smaller proteins containing 104 (for the control structure) and 120 residues (for the wild-type and mutant structures) and explicit water molecules (see Table 2), and ignored non-bonded interactions over 14 Å. These results seem to represent the prominent structural changes with reflecting the short-range interactions. In contrast, the non-periodic systems dealt with larger proteins containing 139 residues (for the wild-type and mutant structures) and approximately 4 times as many water molecules as those of the periodic systems. In addition, all non-bonded interactions in the systems are calculated by using the special purpose computer MDM. Therefore, these would be more suitable results for physiological conditions. We arrived at the following conclusion from a comparison of the periodic and non-periodic results, although they differed with respect to system size, the treatment of non-bonded interactions, and so on.

The β-sheet structure in the globular domain is sensitive to the flexible N-terminal containing dozens of amino acid residues (90-124 or 109-124). The N-terminal of the control structure (125-228) is too short to affect the β-sheet structure despite its flexibility. The flexible and disordered N-terminal of the mutant structure (90-124) changes the structure of the S1 strand and then leads to the extension the β-sheet. Because this extension is observed in both simulations, the phenomenon seems to be intrinsic for the prion protein with the Ala^{117}→Val mutation. The wild-type extra peptide in the periodic system produces the new α-helix in the N-terminal region, but the formation of a new α-helix has not been observed in experiments with prion proteins in different sizes [7] [8] or in the result of the non-periodic system. It will be reasonable to suppose that the wild-type N-terminal region did not promote expansion of the β-sheet.

We speculate that the first stages in the transformation from PrP^{C} to PrP^{SC} by the $Ala^{117}\rightarrow Val$ mutation are as follows. The mutant extra peptide chain induces a structural change in the vicinity of S1 that the paralleling of the two β strands containing S1 and S2 occurs. This results in the extension of the β-sheet accompanied by the destruction of H1.

References

[1] S. B. Prusiner and S. DeArmond, *Annu. Rev. Neurosci.,* **17**, 311-319 (1994).

[2] D. R. Borchelt, M. Scott, A. Taraboulos, N. Stahl and S. B. Prusiner, *J. Cell. Biol.,* **110**, 743-752 (1990).

[3] N. Stahl, M. A. Baldwin, R. Hecker, K. M. Pan, A. L. Burlingame and S. B. Prusiner, *Biochemistry,* **31**, 5043-5053 (1992).

[4] N. Stahl, D. R. Borchelt, K. Hsiao and S. B. Prusiner, *Cell,* **51**, 229-240 (1987).

[5] N. Stahl, M. A. Baldwin, D. B. Teplow, L. Hood, B. W. Gibson, A. L. Burlingame and S. B. Prusiner, *Biochemistry*, **32**, 1991–2002 (1993).

[6] K. M. Pan, M. Baldwin, J. Nguyen, M. Gasset, A. Serban, D. Groth, I. Mehlehorn, Z. Huang, R. J. Fletterick, F. E. Cohen and S. B. Prusiner, *Proc. Natl. Acad. Sci. U.S.A.,* **90**, 10962-10966 (1993).

[7] F. L. Garcia, R, Zahn., R, Riek and K, Wuthrich, *Proc. Natl. Acad. Sci. U.S.A.,* **97**, 8334-8339 (2000).

[8] R. Zahn, A. Liu, T. Luhrs, R. Riek, C. V. Schroetter, F. L. Garcia, M. Billeter, L. Calzolai, G. Wide and K. Wuthrich, *Proc. Natl. Acad. Sci. U.S.A.,* **97**, 145-150 (2000).

[9] K. Hsiao, H. F. Baker, T. J. Crow, M. Poulter, F. Owen, J. D. Terwilliger, D. Westaway, J. Ott and S. B. Prusiner, *Nature,* **338**, 342-345 (1989).

[10] H. A. Kretzschmar, *Arch. Virl. Suppl.,* **7**, 261-293 (1993).

[11] J. Tateishi, T. Kitamoto, K. Dohura, Y. Sakaki, G. Steinmets, C. Tranchant, J. M. Warter and N. Heldt, *Neurology,* **40**, 1578-1581 (1990).

[12] K. K. Hsiao, C. Cass, G. D. Schellenberg, T. Bird, E. Devine-Gage, H. Wisniewski and S. B. Prusiner, *Neurology,* **41**, 681-684 (1991).

[13] J. A. Mastrianni, M. T. Curtis, J. C. Oberholtzer, M. M. Da Costa, S. DeArmond, S. B. Prusiner and J. Y. Garbern, *Neurology,* **45**, 2042-2050 (1995).

[14] C. Tranchant, N. Sergeant, A. Wattez, M. Mohr, J. M. Warter and A. Delacourte, *Journal of Neurology, Neurosurgery, and Psychiatry,* **63**, 240-246 (1997).

[15] D. R. Brown, *Biochem. J.,* **346**, 785-791 (2000).

[16] T. Narumi, A, Kawai and T, Koishi, Proc. SC2001 (Assoc. Comp. Machinery New York) in CDROM (2001).

[17] D. A. Case, D. A. Pearlman, J. W. Caldwell, T. E. Cheatham III, W. S. Ross, C. L. Simmerling, T. A. Darden, K. M. Merz, R. V. Stanton, A. L. Cheng, J. J. Vincent, M. Crowley, D. M. Ferguson, R. J. Radmer, G. L. Seibel, U. C. Singh, P. K. Weiner and P. A. Kollman, AMBER 5, University of California, San Francisco (1997).

[18] D. A. Case, D. A. Pearlman, J. W. Caldwell, T. E. Cheatham III, W. S. Ross, C. L. Simmerling, T. A. Darden, K. M. Merz, R. V. Stanton, A. L. Cheng, J. J. Vincent, M. Crowley, V. Tsui, R. J. Radmer, Y. Duan, J. Pitera, I. Massova, G. L. Seibel, U. C. Singh, P. K. Weiner and P. A. Kollman, AMBER 6, University of California, San Francisco (1999).

[19] W. D. Cornell, P. Cieplak, C. I. Bayly, I. R. Gould, K. M. Merz, Jr., D. M. Ferguson, D. C. Spellmeyer, T. Fox, J. W. Caldwell and P. A. Kollman, *J. Am. Chem. Soc.* **117**, 5179-5197

(1995).
[20] P. Kollman, R. Dixon, W. Cornell, T. Fox, C. Chipot and A. Pohorille, *Computer Simulation of Biomolecular Systems, Vol. 3* A. Wilkinson, P. Weiner, W. Van Gunsteren, eds, Elsevier, 83-96 (1997).
[21] H. J. C. Berendsen, J. P. M. Postma, W. F. van Gunsteren, A. DiNola and J. R. Haak, *J. Chem. Phys.,* **81**, 3684-3690 (1984).
[22] W. L. Jorgensen, J. Chandrasekhar and J. D. Madura, *J. Chem. Phys.,* **79**, 926-935 (1983).
[23] R. A. Laskowski, M. W. MacArthur, D. S. Moss and J. M. Thornton, *J. Appl. Cryst.,* **26**, 283-291 (1993).
[24] R. Koradi, M. Billeter and K. Wuthrich, *J. Mol. Graphics.*, **4**, 51–55 (1996).